

# Electronic Structure of $\text{AlB}_2$ -type U-Si Binary Intermetallic Compounds by Hybrid Density Functional Calculations

Yuting Zhang<sup>1,2</sup>, Pengchuang Liu<sup>3</sup>, Yajiang Xian<sup>1</sup>, Xin Wang<sup>1</sup>, Liusi Sheng<sup>2</sup> and Pengcheng Zhang<sup>1</sup>

1. Science and Technology on Surface Physics and Chemistry Laboratory, Jianguyou 621908, Sichuan, China

2. School of Nuclear Science and Technology, National Synchrotron Radiation Laboratory, University of Science and Technology of China, Hefei 230029, Anhui, China

3. Institute of Materials, China Academy of Engineering Physics, Jianguyou 621908, Sichuan, China

**Abstract:** In this paper the electronic structure of  $\text{AlB}_2$ -type  $\text{USi}_2$  has been explored using DFT, DFT+U and hybrid functional (HSE) methods. It reveals that  $c/a$  has great effect on the electronic structure, particularly the  $f$  orbitals, and there exists strong hybridization between the Si- $p$  and U- $d$  orbitals in  $\text{AlB}_2$ -type  $\text{USi}_2$ . These calculations uncover that there exists similarities on the crystal structure and the electronic structure between  $\text{AlB}_2$ -type  $\text{USi}_2$  and  $\text{U}_3\text{Si}_5$ . Present calculations provide a further insight on the  $\text{U}_3\text{Si}_5$ , a heavy-fermion system.

**Key words:** Electronic structure, heavy-fermion system, U-Si binary system.

## 1. Introduction

Recently, several advanced composite fuels, e.g.  $\text{UN}/\text{U}_3\text{Si}_5$ ,  $\text{UN}/\text{U}_3\text{Si}_2$ ,  $\text{UN}/\text{UB}_4$ , with enhanced thermal conductivity and increased fuel density, have been proposed with uranium nitride as a primary phase to be the candidates in light water reactor [1].  $\text{UN}/\text{U}_3\text{Si}_5$  has a similar thermal and fast flux neutron spectrum to  $\text{UO}_2$  [1, 2]. In particular, the thermal conductivity of  $\text{U}_3\text{Si}_5$  at room temperature is ac. 60% lower than  $\text{UO}_2$ ; on heating, the thermal conductivity of  $\text{U}_3\text{Si}_5$  overtakes the value of  $\text{UO}_2$  at 574 K and continues to increase with temperature [2]. In addition, there exists an unknown phase transformation around 723 K, which contradicts with the present U-Si binary phase diagram. To better understand the physical properties of  $\text{U}_3\text{Si}_5$ , it is essential to understand the electronic interaction between Si and U element.

The electronic interaction between Si and U element has been investigated during the past several decades. The U-Si binary intermetallic compounds can be classified into 3 groups, heavy-fermion system, magnetically ordered one and paramagnetic one [3].  $\text{U}_3\text{Si}_5$  is a heavy-fermion system with  $\mu_{\text{eff}}=3.46 \mu_B/\text{U}$  and  $\gamma = 120 \text{ mJ}/\text{K}^2\text{U-mol}$ ;  $\text{USi}$  is of ferromagnetic order but with *ca.*  $0.1 \mu_B/\text{U}$ ;  $\text{U}_3\text{Si}$ ,  $\text{U}_3\text{Si}_2$  and  $\text{USi}_3$  are all Pauli paramagnetic ones. Up to now, there is no definite conclusion on the magnetic properties on  $\text{AlB}_2$ -type  $\text{USi}_2$ . Interestingly,  $\text{U}_3\text{Si}_5$  was considered as a deficiency structure of  $\text{AlB}_2$ -type  $\text{USi}_2$  [4]. These results suggest that the itinerant or localized property of the  $5f$  electrons depends on both the U-U and the U-Si distances. Earlier valence band spectrum by XPS (X-ray photoemission spectroscopy) and BIS (bremsstrahlung-isochromat spectroscopy) [5] has shown that  $\text{U}_3\text{Si}_2$ ,  $\text{USi}$ ,  $\text{USi}_2$ , and  $\text{USi}_3$ , transform from the direct  $f$ - $f$  interaction to only  $f$ -lig and interactions, suggesting  $f$ -band broadening with increasing ligand interactions. Fujimori et al. [6, 7]

---

**Corresponding author:** Xin Wang, Dr., assistant professor, research field: computational condensed matter physics;

Pengcheng Zhang, Dr., professor, research field: nuclear materials.

found an unknown ordered phase when the U film, deposited on the Si(100) and Si(111), was annealed at 973 K. Recently, Chen et al. [4] performed the same experiment again but annealed at 870 K. They obtained an ordered hexagonal phase too, and then confirmed the unknown phase to be U<sub>3</sub>Si<sub>5</sub> phase by using STM (scanning tunneling microscopy), LEED (lowenergy electron diffraction) and RHEED (reflection high energy electron diffraction).

Here, through first-principles calculations within the framework of standard density functional theory (DFT), DFT + U with U<sub>eff</sub> from 1 to 4 and hybrid functional (HSE) [8, 9] by including the nonlocal exchange-interaction effect in combination with charge density topology analysis, we have calculated the electronic structure of AlB<sub>2</sub>-type USi<sub>2</sub>. Our results agree well with the previous experimental findings, i.e., valence band structure by XPS. The paper is organized as follows. The computational methods are described in Section 2. Results and discussions of the density functional calculations are provided in Section 3. Lastly, concluding remarks are presented in Section 4.

## 2. Computational Method

The VASP (Vienna *ab initio* Simulation Package) [10-12] was employed by utilizing the PAW (projector augmented wave) method [13, 14] within the framework of DFT (density functional theory) [15, 16]. The PBE (Perdew-Becke-Ernzerh) of exchange-correlation functional implementation of the GGA (generalized gradient approximation) was used. The semicore  $6s^2 6p^6 5f^3 6d^1 7s^2$  of U and the valence state  $3s^2 3p^2$  of Si were included in the PAW potentials. Tests of the energy convergence with respect to the k-point mesh size and energy cut-off led to the choice of an energy cut-off of 500 eV and a gamma-centered Monkhorst-Pack k-point mesh corresponding to a  $15 \times 15 \times 15$  mesh for AlB<sub>2</sub>-type crystal structures. Internal energies were converged with respect to the energy cut-off and k-point mesh to within 0.1 meV. For a

single-point calculation the tetrahedron method with Blöchl correction method [17] was employed.

It is well-known that U often exhibits the localized *f*-electronic states, hence the hybrid functional [8, 9] was introduced to calculate the total energies and electronic structure. The HSE employs an admixture of Hartree-Fock-like nonlocal exchange interaction and PBE exchange in the construction of the many-body exchange (x) and correlation (c) functional as follows,

$$E_{xc}^{HSE} = \alpha E_x^{HF, sr, \mu} + (1-\alpha) E_x^{PBE, sr, \mu} + E_x^{PBE, lr, \mu} + E_c^{PBE} \quad (1)$$

where (sr) and (lr) refer to the short- and long-range parts of the respective exchange interactions, whereas  $\mu$  controls the range separation of the Coulomb kernel, varying between 0.2 and 0.3 Å<sup>-1</sup>. We used the generally adopted value of  $\mu = 0.2$  Å<sup>-1</sup> [18]. The HSE functional is largely self-interaction free thus improving over the standard DFT description. Present calculations un-covers that the electronic structure of Diamond-type Si can be described well within the HSE framework. The valence band spectrum derived within HSE framework with  $\alpha = 0.25$  reproduces experimental findings [4, 19], as shown in Fig. 1. In addition, the band gap of Si derived within DFT is 0.67 eV, while that obtained within HSE with  $\alpha = 0.25$  equals 1.2 eV, which agrees well with the experimental value 1.1 eV.

For AlB<sub>2</sub>-type USi<sub>2</sub> binary intermetallic compounds, the calculations within the HSE06 framework with different mixture parameter were performed using a  $9 \times 9 \times 9$  *k*-mesh sampling. For comparison, we also introduced the DFT+*U* method with  $J = 0.51$  and the Hubbard parameter U<sub>eff</sub> ranging from 1 to 4.

## 3. Results and Discussions

### 3.1 The Structure of AlB<sub>2</sub>-type USi<sub>2</sub>

The optimized lattice parameters of AlB<sub>2</sub>-type USi<sub>2</sub> and U<sub>3</sub>Si<sub>5</sub> are presented in Table 1. For USi<sub>2</sub> with  $c/a < 1.0$ , it can be seen that the standard DFT can give a good description of USi<sub>2</sub>, with the error within 1%,

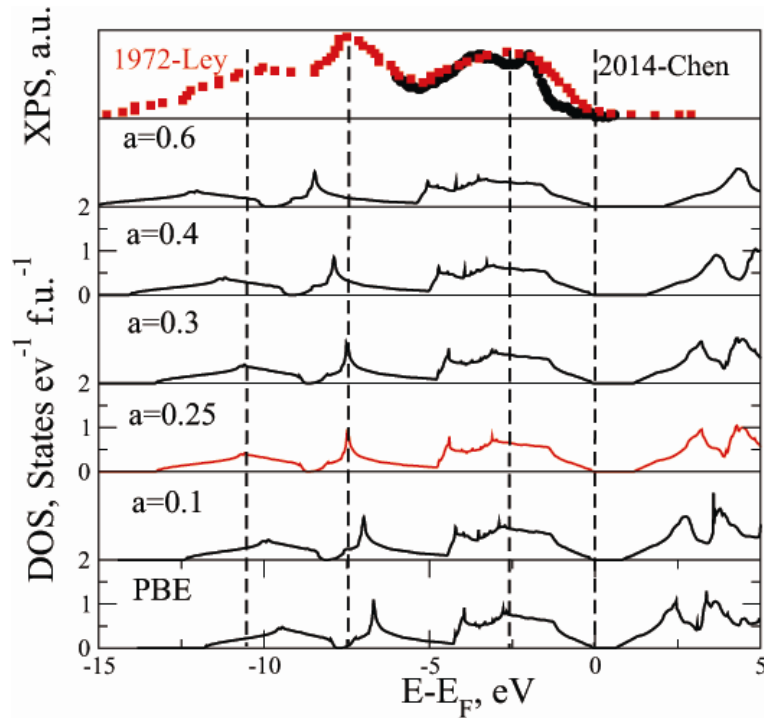


**Fig. 1** (color online) The valence band spectrum of Si: theoretical calculations within DFT and HSE framework and experimental findings. The red squares is from Ref. [19] and black circles is from Ref. [4].

**Table 1** The optimized structural parameters (lattice constant in Å and  $c/a$ ) and magnetic properties for AIB<sub>2</sub>-type USi<sub>2</sub> and Diamond-type Si, as well as available experimental results.

	Space group	$a$	$c$	$c/a$	mag/ $\mu_B/U$	Method
USi <sub>2</sub>	P6/mmm	4.0053	3.7839	0.945	-	DFT
USi <sub>2</sub>	P6/mmm	4.0387	3.8583	0.9553	1.917	DFT + U1
USi <sub>2</sub>	P6/mmm	4.0156	4.1226	1.027	2.391	DFT + U2
USi <sub>2</sub>	P6/mmm	4.0490	4.2196	1.042	2.699	DFT + U3
USi <sub>2</sub>	P6/mmm	4.0728	4.2631	1.047	2.839	DFT + U4
USi <sub>2</sub>	P6/mmm	4.0384	3.7835	0.937	-	PW91 [21]
USi <sub>2</sub>	P6/mmm	4.028	3.852	0.956	-	Expt [22]
U <sub>3</sub> Si <sub>5</sub>	P6/mmm	3.843	4.096	1.059	3.46	Expt [22]
USi <sub>2</sub>	P6/mmm	4.020	3.827	0.952	2.190	$\alpha = 0.1$
USi <sub>2</sub>	P6/mmm	3.978	4.090	1.028	2.540	$\alpha = 0.25$
USi <sub>2</sub>	P6/mmm	3.999	4.239	1.060	3.34	$\alpha = 0.4$
USi <sub>2</sub>	P6/mmm	3.975	4.020	1.011	2.023	$\alpha = 0.6$
Diamond-Si	Fd-3m	5.4349	-	-	-	$\alpha = 0.25$
Diamond-Si	Fd-3m	5.4686	-	-	-	DFT
Diamond-Si	Fd-3m	5.4309	-	-	-	Expt [23]

compared with experimental results. The lattice parameter derived within DFT+ $U$  with  $U_{eff}=1$  and the HSE framework with  $\alpha=0.1$  can give more accurate description. For USi<sub>2</sub> with  $c/a > 1.0$ , the lattice parameters derived within DFT+ $U$  with  $U_{eff}=2$  are much larger with the error 4.5% and 0.6%,

respectively, as compared with the experimental findings. Moreover, the larger the  $U_{eff}$ , the larger difference with experimental results. The lattice parameter obtained within HSE with  $\alpha=0.25$  give the best description. These calculations reveal that standard DFT can find the USi<sub>2</sub> with  $c/a < 1.0$ ; the

Hubbard parameter  $U$  has significant effect on the lattice parameter; the hybrid functionals with proper value of mixture parameter can find the USi<sub>2</sub> with  $c/a > 1.0$ .

Fig. 2 shows the simulated XRD patters of powder samples of AlB<sub>2</sub>-type USi<sub>2</sub> with  $c/a > 1.0$  and  $c/a < 1.0$ , respectively. It shows that  $c/a$  has obvious effect on the XRD patters. For example, in contrast to USi<sub>2</sub> with  $c/a < 1.0$  (see Fig. 2a), the peak of (001) at ca. 22 degree shifts to a lower angle, while the peak of (100) at ca. 25 degree shifts to a higher angle (see Fig. 2b). Here, it should note that the peak positions are determined by the crystal structure, while the peak intensities are mainly dependent on the structure factors. In this sense, these observations can be rationalized. Since the interplanar spacing of (001) for USi<sub>2</sub> with  $c/a > 1.0$  (4.096 Å) is higher than that of USi<sub>2</sub> with  $c/a < 1.0$  (3.852 Å), thus the (001) peak is lowered to lower angle. Conversely, the interplanar spacing of (100) for USi<sub>2</sub> with  $c/a > 1.0$  (3.328 Å) is lower than that of USi<sub>2</sub> with  $c/a < 1.0$  (3.488 Å), therefore, the (001) peak is lifted to higher angle.

It also should note that the simulated XRD of AlB<sub>2</sub>-type USi<sub>2</sub> with  $c/a > 1.0$  is consistent with the experimental findings of U<sub>3</sub>Si<sub>5</sub> [2], suggesting that the Si vacancy may have little effect on the XRD pattern. These observations uncover that there exist similarities between the AlB<sub>2</sub>-type USi<sub>2</sub> with  $c/a > 1.0$  and the U<sub>3</sub>Si<sub>5</sub>. Thereafter, the electronic structure of AlB<sub>2</sub>-type USi<sub>2</sub> with  $c/a > 1.0$  may provide further insight on the heavy-fermion behavior of U<sub>3</sub>Si<sub>5</sub>.

### 3.2. The Electronic Structure of AlB<sub>2</sub>-type USi<sub>2</sub>

First of all, the electronic structure within both standard DFT and HSE frameworks are calculated. For comparison, the available experimental findings are also plotted (see Fig. 3). The electronic structure derived within HSE frameworks with  $\alpha = 0.25$  is in agreement with valence band spectrum determined by experiment [5, 7], suggesting that the exchange-correlation in AlB<sub>2</sub>-type USi<sub>2</sub> is reliable. This is also consistence with previous calculation results of Si within HSE framework.

Then, the total DOS derived within DFT and HSE

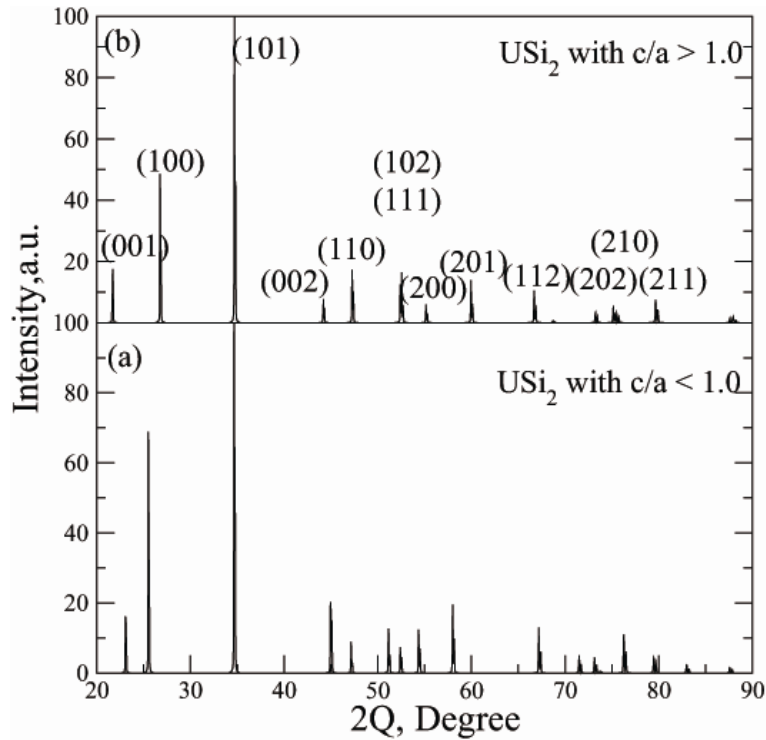
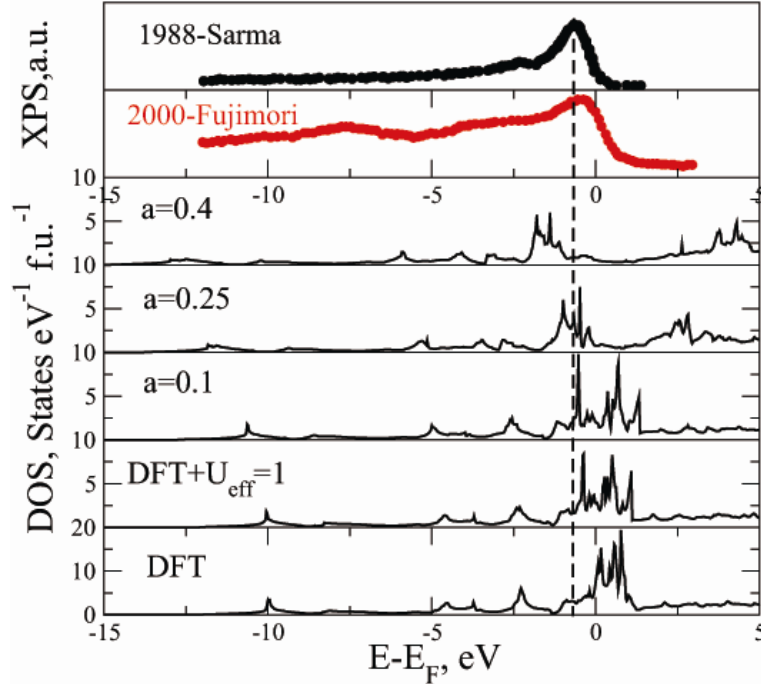


Fig. 2 The simulated XRD patter of powder sample. (a) AlB<sub>2</sub>-type USi<sub>2</sub> with  $c/a < 1.0$  (b) AlB<sub>2</sub>-type USi<sub>2</sub> with  $c/a > 1.0$ . The lattice parameters are from experimental value, as shown in Table 1.



**Fig. 3** (color online) The valence band spectrum of  $\text{USi}_2$ : Theoretical calculations within DFT, DFT+ U and HSE frameworks and experimental findings. The black circles is from Ref. [5] while the red diamonds is from Ref. [7], derived after annealed at 973 K. The vertical dashed line are provided to guide the eye.

are shown in Fig. 4. It shows that for  $\text{AlB}_2$ -type  $\text{USi}_2$  with  $c/a > 1.0$  the main peaks obtained within HSE shift to lower energy level; particularly, the DOS at fermi level ( $E_F$ ) shrink to a peak just below the  $E_F$  (see Fig. 4a), evidencing the strong electronic correlation in this crystal system. For  $\text{AlB}_2$ -type  $\text{USi}_2$  with  $c/a < 1.0$ , the main peaks at  $E_F$  obtained within standard DFT split into two peaks separated by  $E_F$  and the DOS at  $E_F$  drastically decrease (see Fig. 4b). Fig. 5 shows the projection DOS of  $\text{AlB}_2$ -type  $\text{USi}_2$ . It shows that the  $p$  and  $d$  orbitals have similar peak site, suggesting the hybridization between these orbitals. It also shows that  $c/a$  has a great effect on the electronic structure, particularly the  $f$  orbitals. For  $\text{AlB}_2$ -type  $\text{USi}_2$  with  $c/a > 1.0$ , the  $f$  orbitals just locate below the  $E_F$  (see Fig. 5a), while for  $\text{AlB}_2$ -type  $\text{USi}_2$  with  $c/a < 1.0$ , the  $f$  orbitals split into two main peaks below the  $E_F$  (see Fig. 5b). It should note that the DOS for spin-up and spin-down are not symmetric, thus, the U atom in these two crystal structures should exhibit magnetic moments (ca.  $2.5 \mu_B/\text{U-atom}$ ), congruent with experimental findings ( $3.2\text{-}3.5 \mu_B/\text{U-atom}$ ) [3, 20].

Further, the band structure of these two crystal structures within HSE framework are presented, as shown in Figs. 6 and 7, respectively. For these two  $\text{AlB}_2$ -type  $\text{USi}_2$  crystal structures Si-3s and U- $p$  electrons share the same band at lower energy level, while Si-3p and U- $d$  electrons occupy the same band at higher energy level, suggesting two hybridizations, i.e. Si-3/U- $p$  hybridization and Si-3p/U- $d$  hybridization. The occupancy of  $f$  bands in  $\text{AlB}_2$ -type  $\text{USi}_2$  are similar but with a little difference. For  $\text{USi}_2$  with  $c/a < 1.0$ , there is a near flat  $f$  bands along  $K\text{-}\Gamma\text{-}M$  direction, while for  $\text{USi}_2$  with  $c/a > 1.0$ , there is a strong hybridization between the Si- $p$  and U- $d$  electrons along  $K\text{-}\Gamma\text{-}M$  direction. The band structure of  $\text{AlB}_2$ -type  $\text{USi}_2$  with  $c/a > 1.0$  derived by ARPES [4] revealed three bands (marked by A, B and C, respectively) along  $\Gamma\text{-}M$  direction, but no  $f$  bands. They explained this due to the high intensity of U-5f states and strong hybridization of U-5f and U-6d orbitals near the  $E_F$ . Since the experimental results above are not spin-resolved, thus, it should be explained by the combination of the calculation results

of spin-up and spin-down. Here, these calculations reveal that the A bands belongs to U- $p$ , while the B

and C bands belong to the hybridization of U- $p$ /U- $d$  and the hybridization of U- $p$ /U- $d$ /Si- $p$ , respectively.

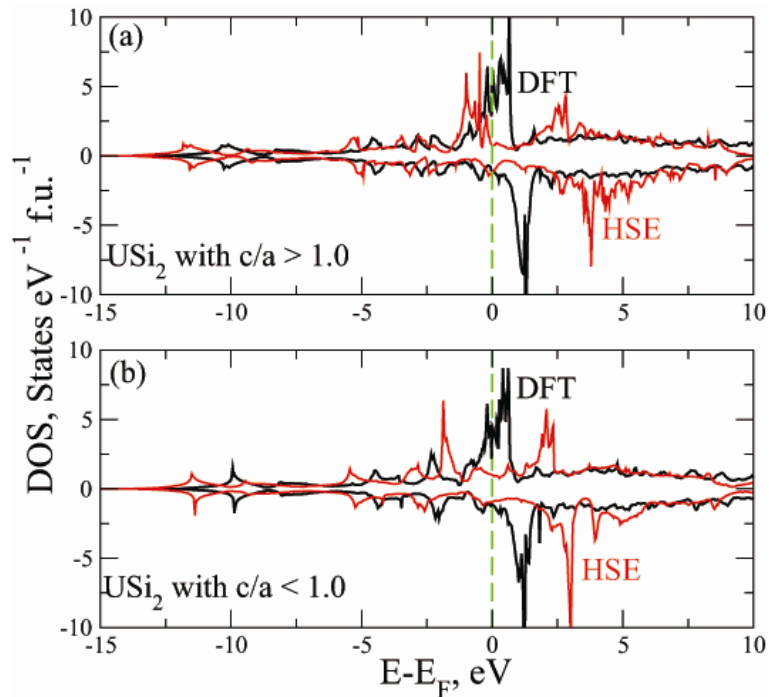


Fig. 4 (color online) The electronic structure of  $AIB_2$ -type  $USi_2$  within DFT and HSE with  $\alpha = 0.25$ . (a)  $USi_2$  with  $c/a > 1.0$  (b)  $USi_2$  with  $c/a < 1.0$ .

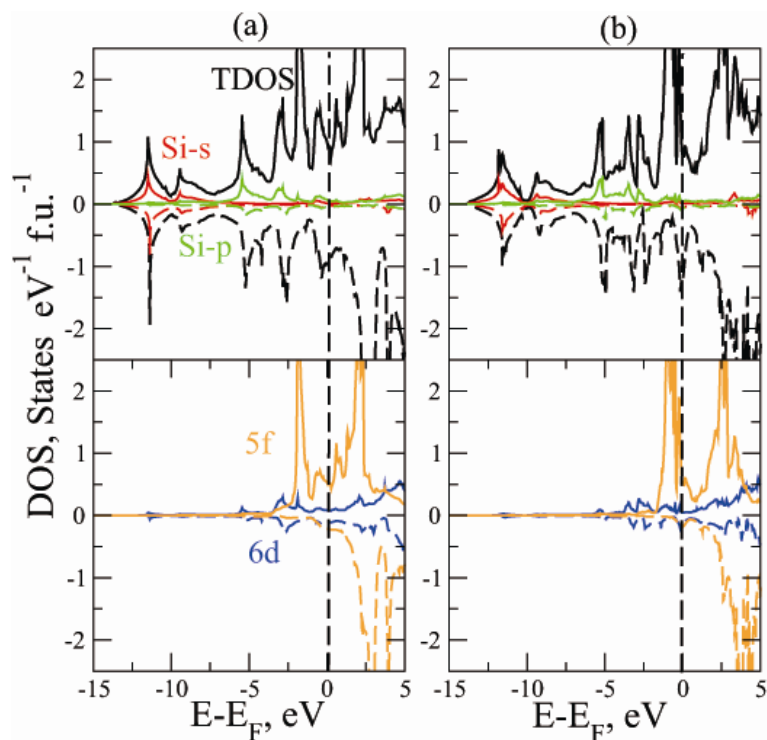


Fig. 5 (color online) pDOS of  $AIB_2$ -type  $USi_2$  within HSE with  $\alpha = 0.25$  (a)  $c/a < 1$  (b)  $c/a > 1$ .

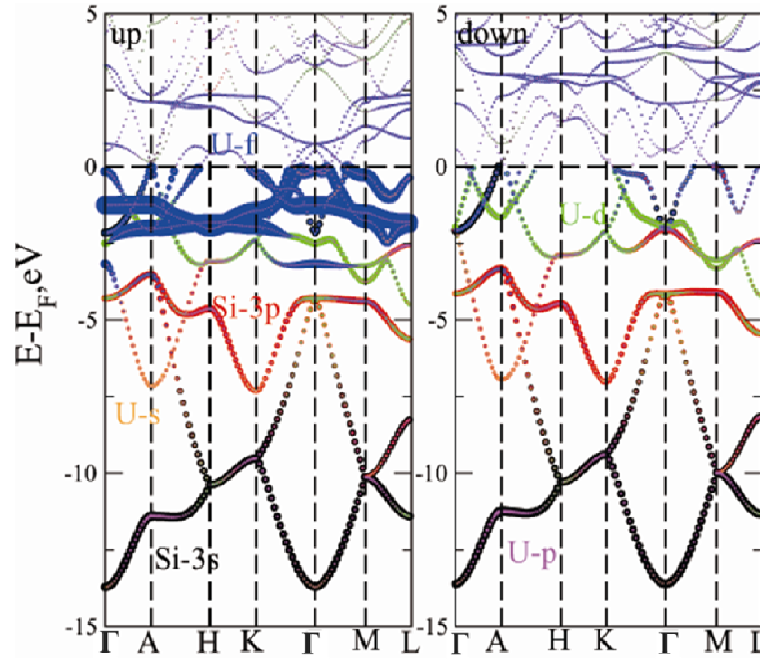


Fig. 6 Band structure of  $AlB_2$ -type  $USi_2$  with  $c/a < 1.0$  derived within HSE framework with  $\alpha = 0.25$ .

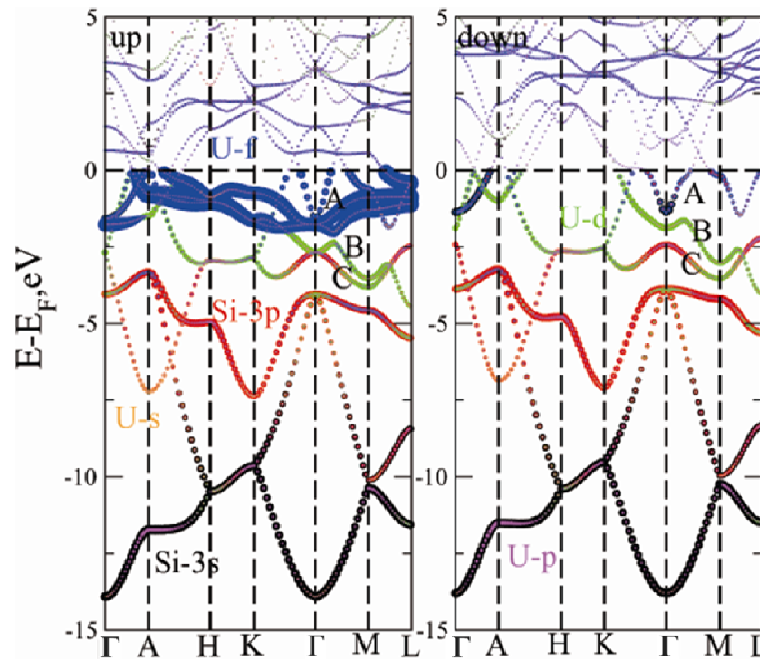


Fig. 7 Band structure of  $AlB_2$ -type  $USi_2$  with  $c/a > 1.0$  derived within HSE framework with  $\alpha = 0.25$ .

#### 4. Conclusions

In summary, we have investigated the electronic structure of  $AlB_2$ -type U-Si binary intermetallic compounds using first-principles calculations. There are two  $AlB_2$ -type crystal structures with different  $c/a$ . The electronic structure of  $AlB_2$ -type  $USi_2$  is similar

with that of  $U_3Si_5$ . Hybrid functional can greatly improve the description of exchange-correlation functionals for these two structures. The strong electronic correlation in  $AlB_2$ -type  $USi_2$  with  $c/a > 1.0$  is evidenced by the shrinkage in the DOS by comparison of DOS derived within DFT and HSE frameworks. Present calculations provide a new

insight on the heavy-fermion behavior of  $\text{U}_3\text{Si}_5$ .

## Acknowledgments

This work was supported by NSFC under the grant No. 91226203. We also acknowledged the financial support by Science and Technology on STSPCL (Surface Physics and Chemistry Laboratory) under the grant No. ZDXKFZ201410.

The authors declare no conflict of interest.

## References

- [1] Brown, N. R., Aronson, A., Todosow, M., Brito, R., and McClellan, K. J. 2014. "Neutronic Performance of Uranium Nitride Composite Fuels in a PWR." *Nucl. Eng. Design* 275: 393-407.
- [2] White, J., Nelson, A., Byler, D., Safarik, D., Dunwoody, J., and McClellan, K. 2015. "Thermophysical Properties of  $\text{U}_3\text{Si}_5$  to 1773 K." *J. Nucl. Mater.* 456: 442-8.
- [3] Miyadai, T., Mori, H., Oguchi, T., Tazuke, Y., Amitsuka, H., Kuwai, T., and Miyako, Y. 1992. "Magnetic and Electrical Properties of the U-Si System." *J. Mag. Mag. Mater.* 104C107, Part 1: 47-8.
- [4] Chen, Q., Yang, Y., Feng, W., and Lai, X. 2014. "Formation of Two-Dimensional Uranium Silicide Film and Its Electronic Structure Study." *Physica B* 436: 215-9.
- [5] Sarma, D., Krummacher, S., Hillebrecht, F., and Koelling, D. 1988. "5*f*-Band Width and Hybridization in Uranium Silicides." *Phys. Rev. B* 38: 1.
- [6] Fujimori, S.-i., Saito, Y., Yamaki, K.-i., Okane, T., Sato, N., Komatsubara, T., Suzuki, S., and Sato, S. J. 1998. *Elec. Spectr. Related Phenom.* 88: 631-5.
- [7] Fujimori, S., Saito, Y., Yamaki, K., Okane, T., Sato, N., Komatsubara, T., Suzuki, S., and Sato, S. 2000. "Photoemission Study of the U/Si (111) Interface." *Surf. Sci.* 444: 180-6.
- [8] Heyd, J., Scuseria, G. E., and Ernzerhof, M. 2006. "Hybrid Functionals Based on a Screened Coulomb Potential." *J. Chem. Phys.* 124: 219906.
- [9] Paier, J., Marsman, M., Hummer, K., Kresse, G., Gerber, I. C., and Angyan, J. G. 2006. "Screened Hybrid Density Functionals Applied to Solids." *J. Chem. Phys.* 124: 154709.
- [10] Kresse, G., and Hafner, J. 1993. "Ab Initio Molecular Dynamics for Liquid Metals." *Phys. Rev. B* 47: 558.
- [11] Kresse, G., and Furthmüller, J. 1996. "Efficiency of Ab-initio Total Energy Calculations for Metals and Semiconductors Using a Plane-Wave Basis Set." *Comput. Mater. Sci.* 6: 15-50.
- [12] Kresse, G., and Furthmüller, J. 1996. "Efficient Iterative Schemes for Ab Initio Total-Energy Calculations Using a Plane-Wave Basis Set." *Phys. Rev. B* 54: 11169.
- [13] Blöchl, P. E. 1994. "Projector Augmented-Wave Method." *Phys. Rev. B* 50: 17953.
- [14] Kresse, G., and Joubert, J. 1999. "From Ultrasoft Pseudopotentials to the Projector Augmented-Wave Method." *Phys. Rev. B* 59: 1758.
- [15] Hohenberg, P., and Kohn, W. 1964. "Inhomogeneous Electron Gas." *Phys. Rev.* 136: 864-71.
- [16] Kohn, W., and Sham, L. 1965. "Self Consistent Equations Including Exchange Correlation Effects." *J. Phys. Rev.* 140: A1133.
- [17] Blochl, P. E., Jepsen, O., and Andersen, O. K. 1994. "Improved Tetrahedron Method for Brillouin-Zone Integrations." *Phys. Rev. B* 49: 16223.
- [18] Xing, W., Liu, P., Cheng, X., Niu, H., Ma, H., Li, D., Li, Y., Chen, X.-Q. 2014. "Vacancy Formation Enthalpy of Filled D-Band Noble Metals by Hybrid Functionals." *Phys. Rev. B* 90: 144105.
- [19] Ley, L., Kowalczyk, S., Pollak, R., and Shirley, D. A. 1972. "X-Ray Photoemission Spectra of Crystalline and Amorphous Si and Ge Valence Bands." *Phys. Rev. Lett.* 29: 1088-92.
- [20] Remschnig, K., Bihan, T. L., Noel, H., and Rogl, P. 1992. "Structural Chemistry and Magnetic Behavior of Binary Uranium Silicides." *J. Solid State Chem.* 97: 391-9.
- [21] Yang, J., Long, J., Yang, L., and Li, D. 2013. "First-Principles Investigations of the Physical Properties of Binary Uranium Silicide Alloys." *J. Nucl. Mater.* 443: 195-9.
- [22] Brown, A., and Norreys, J. 1961. "Uranium Disilicide." *Nat.* 191: 61-2.
- [23] Straumanis, M., and Aka, E. 1952. "Lattice Parameters, Coefficients of Thermal Expansion, and Atomic Weights of Purest Silicon and Germanium." *J. Appl. Phys.* 23: 330-4.